



Intercontinental Geoinformation Days

igd.mersin.edu.tr



Photogrammetric analysis of multispectral and thermal close-range images

Özgün Akçay*¹

¹Canakkale Onsekiz Mart University, Faculty of Engineering, Department of Geomatics Engineering, Canakkale, Turkey

Keywords

Photogrammetry
Remote sensing
Multispectral images
Thermal images
Close-range

ABSTRACT

Sensors capable of multispectral and thermal imaging beyond visible bands offer many analysis possibilities for environmental monitoring. Different sensor images constitute an important source of information especially in the fields of agriculture, forestry, geology and energy. Photogrammetric studies have been affected by this development in recent years and have been used in the production of multispectral and thermal models besides the RGB model. However, due to geometric and radiometric resolution differences, it is difficult to combine or evaluate models produced from different types of sensors. In this study, the three-dimensional test field images obtained with RGB, multispectral and thermal sensors were oriented and modeled photogrammetrically. The accuracies of the control points on the produced models were compared and discussed. When the results are examined, control point accuracy was obtained as almost similar as in the RGB model after the orientation based on automatic feature matching. Automatic feature detection and matching in thermal images were not robustly produced due to low geometric resolution. For this reason, manual measurements were performed in thermal images, and the photogrammetric orientation and adjustment process was done accordingly.

1. INTRODUCTION

Recently, multi-sensor modeling and analyzes have been carried out with terrestrial and UAV-based close-range photogrammetry. Although multispectral and thermal lightweight cameras are relatively low resolution compared to RGB cameras, photogrammetric products three-dimensional models and orthophotos have been considered for monitoring and inspection in many areas such as forestry, agriculture and archaeology.

The multispectral data were processed with a photogrammetric pipeline to create triband orthoimages to extract some Vegetation Indices (VI) such as the Normalized Difference Vegetation Index (NDVI), the Green Normalized Difference Vegetation Index (GNDVI), and the Soil Adjusted Vegetation Index (SAVI), examining the vegetation vigor for each crop (Candiago et al., 2015). Saura et al. (2019) also analysed a vineyard with UAV based multispectral imagery and produced the Digital Elevation Model and NDVI to collect information about the agricultural production such as moisture and biomass density. Minařík & Langhammer (2016) proposed a methodology for assessment of spatial and

qualitative aspects of forest disturbance based on the multispectral sensor Tetracam camera with the UAV photogrammetry.

On the other hand, photogrammetric studies which consider both RGB and thermal images are seen. Ribeiro-Gomes et al. (2017) evaluated the use of the Wallis filter for improving the quality of the thermal photogrammetry process using structure from motion software. Despite the low resolution of the thermal imagery compared to RGB imagery, forest structural elements were extracted using both point clouds (Webster et al. 2018). Van der Sluijs et al. (2018) revealed the morphology and daily to annual dynamics of thaw-driven mass wasting phenomenon using photogrammetric terrain models and orthomosaic time series. Zefri et al. (2018) studied about the use of thermal and visual imagery taken by UAV in the inspection of photovoltaic installations. Biass et al. (2019) provided detail in characterizing the emplacement of a compound pāhoehoe lava flow using SfM photogrammetry techniques to visible and thermal data sets.

Studies in which multispectral and thermal three-dimensional photogrammetric models and their analysis

* Corresponding Author

*akçay@comu.edu.tr ORCID ID 0000-0003-0474-7518

Cite this study

Akçay Ö (2021). Photogrammetric analysis of multispectral and thermal close-range images. 2nd Intercontinental Geoinformation Days (IGD), 230-233, Mersin, Turkey

are performed together can also be found in the literature. Erenoglu et al. (2017) developed a novel methodology extracting and distinguishing material features from UAV-based multi-sensor data photogrammetry for the cultural heritages. Edelman (2018) explored the feasibility to obtain visible, infrared, hyperspectral and thermal 3D registrations of simulated crime scenes using photogrammetry for use in forensic practice. Raeva et al. (2019) carried out unmanned flights with a fixed-wing platform with two different sensors – multispectral and thermal in order to examine two main crops cultivated area. Turner et al. (2020) investigated geological discontinuities in hard rock masses using UAV-mounted thermal and multispectral cameras.

In this study, the three-dimensional test field images obtained with RGB, multispectral and thermal sensors were oriented photogrammetrically and the accuracies of the control points on the obtained models were compared. In particular, the effects of sensors on photogrammetry as a result of modeling with multispectral and thermal images were discussed.

2. METHOD

All photogrammetric experiments were carried out on the three-dimensional test field as shown in Fig. 1. There are coded targets of Photomodeler and Agisoft Metashape software on the test area in dimensions of 85 cm x 85 cm x 20 cm. As indicated in the workflow in Fig. 2, firstly, the coordinates of the control points were calculated on the test field. Then, photogrammetric models were created by taking test field images with Sony visible range, Mapir multispectral and Optris thermal cameras. The features of the cameras used in the study are shown in Table 1. Although the resolutions of RGB cameras and multispectral cameras are close to each other, it is seen that the resolution of the thermal camera is quite low compared to the others. In the results section, the accuracies produced from photogrammetric models are presented.

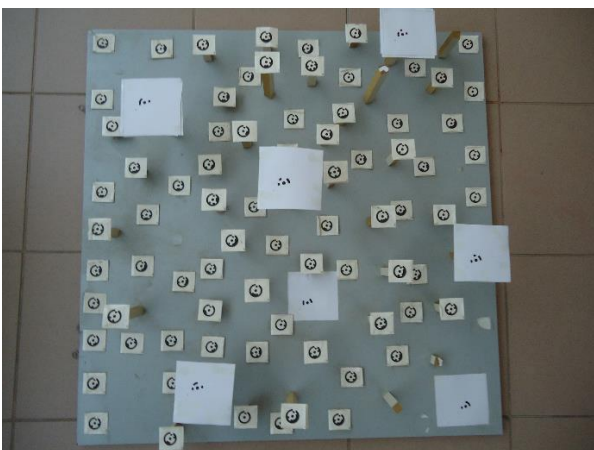


Figure 1. Three dimensional test field

Table 1. Sensor specifications

Name	Band type	Resolution (pixel)
Sony	Red Green Blue	4320 x 3240
Mapir	Orange Cyan NIR	4000x3000
Optris	Thermal	382 x 288

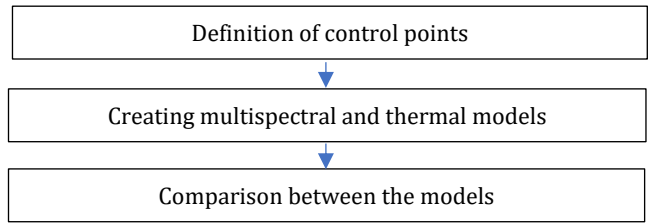


Figure 2. Workflow for photogrammetric analysis

2.1. Photogrammetric Control Points

The coordinates of the control points were also produced by the photogrammetric method. By using 10 images taken with the RGB camera, 75 coded targets were automatically measured with Photomodeler, then the orientation and bundle adjustment processes were completed. Measurements of 7 coded targets (CP1, CP2, CP4, CP6, CP8, CP10 and CP12) belonging to Agisoft software were performed by manual photogrammetric method and model coordinates were generated. After the distance between the targets P1 and P8 was determined with a precision ruler, the model coordinate system was transformed into the local coordinate system defined in the metric system. In Agisoft software, 10 image orientations were re-processed with coded targets, and X, Y, Z coordinates of control points and their errors were defined (Table 2). It is seen that the point location accuracies are about 1 mm.

Table 2. Control points in the local coordinate system

No	X (m)	Y (m)	Z (m)	Error (m)
CP1	0.3750	-0.2895	-0.8057	0.0009
CP2	0.3557	0.0122	-0.6887	0.0013
CP4	0.0197	0.1448	-0.6212	0.0013
CP6	-0.1406	-0.2054	-0.6868	0.0011
CP8	0.0570	-0.0760	-0.8068	0.0012
CP10	0.2448	0.4398	-0.7356	0.0012
CP12	-0.2293	0.3003	-0.6830	0.0013

2.2. Multispectral and Thermal Models

First, radiometric calibration of the multispectral camera images was performed. The 12 images obtained as a result of the calibration were automatically oriented and optimized by the coded targets in Agisoft software. In addition, dense point clouds were produced (Fig. 3).



Figure 3. Multispectral dense cloud point

Since the spectral range of thermal camera images is different than RGB and multispectral sensor images, it was not possible to automatically measure the coded targets in the Agisoft software. Due to noise and radiometric distortions on the thermal images, automatic feature detection and matching was not sufficient for orientation. Fig. 4 shows the views of the same features on different thermal images. 7 coded targets and 11 other targets were manually measured on 13 thermal images. The selectivity of some targets for manual measurements has been increased by coins.

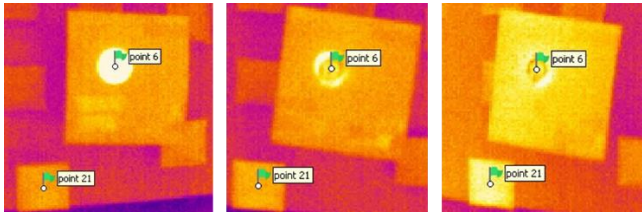


Figure 4. Same features on different thermal images

Fig. 5 explicitly depicts distortions and photogrammetric measurements points in a thermal image. By measuring a total of 18 common points on the images, orientation and optimization were implemented. Dense point clouds could not be produced due to insufficient automatic matching based on the thermal image.

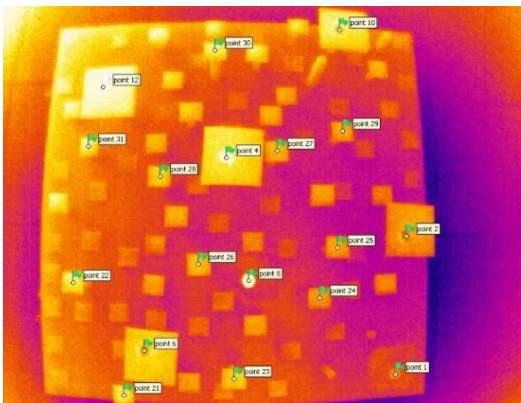


Figure 5. A thermal image and measurement points

3. RESULTS AND DISCUSSIONS

When pixel errors were examined in Table 3 and Fig. 6, it is seen that photogrammetric measurement accuracies are similar in all image types. In other words, the accuracy of manual measurements made in thermal and automatic measurements on RGB and multispectral images produced similar results. In some control points, it is also observed that manual thermal measurements are better than automatic multispectral measurements.

Table 3. Errors of control points in pixel unit

No	RGB	Multispectral	Thermal
CP1	0.231	0.343	0.523
CP2	0.276	0.476	0.29
CP4	0.215	0.293	0.278
CP6	0.252	0.558	0.29
CP8	0.192	0.144	0.334
CP10	0.174	0.299	0.337
CP12	0.289	0.598	0.386

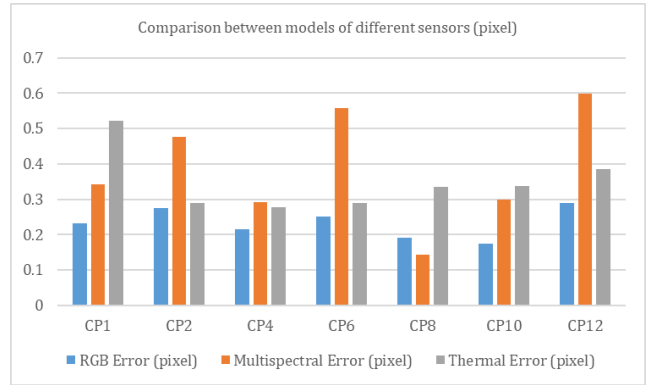


Figure 6. Comparison between in pixel unit

However, when metric accuracies are analyzed in Table 4 and Fig. 7, it is seen that RGB and multispectral results differ significantly from thermal results. Although RGB stands out in terms of accuracy, the results obtained from multispectral images are also very consistent. This is due to the fact that one pixel size of the thermal camera sensor is larger than other sensors.

Table 4. Errors of control points in millimeter unit

No	RGB	Multispectral	Thermal
CP1	0.9	1.7	2.9
CP2	1.3	1.6	3.5
CP4	1.3	1.1	3.1
CP6	1.1	0.7	4.8
CP8	1.2	1.2	1.5
CP10	1.2	1.3	1.8
CP12	1.3	1.5	1.7

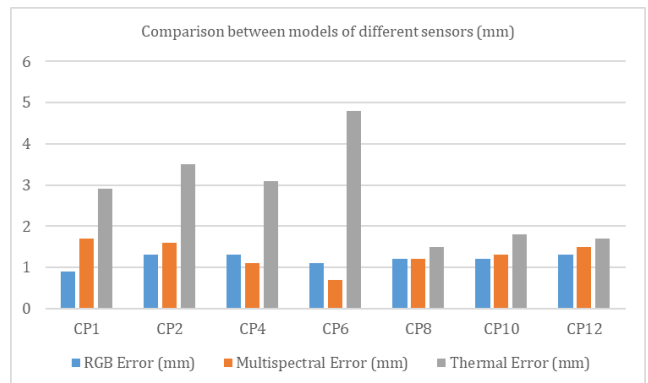


Figure 7. Comparison between errors in millimeter unit

4. CONCLUSIONS

In photogrammetry, besides three-dimensional RGB models, multispectral and thermal models are also successfully produced. In particular, radiometric corrections on multispectral and thermal images are important in terms of geometric positioning accuracy. Due to the difficulties in automatic processing of thermal images, manual point measurement is mandatory, so there is a loss of time and accuracy in model production. The low resolution of thermal images makes it difficult to combine and analyze them with RGB and multispectral models. In the future, studies should be carried out to increase the resolution of thermal models with RGB and multispectral camera images.

REFERENCES

- Ribeiro-Gomes, K., Hernández-López, D., Ortega, J. F., Ballesteros, R., Poblete, T., & Moreno, M. A. (2017). Uncooled thermal camera calibration and optimization of the photogrammetry process for UAV applications in agriculture. *Sensors*, 17(10), 2173.
- Webster, C., Westoby, M., Rutter, N., & Jonas, T. (2018). Three-dimensional thermal characterization of forest canopies using UAV photogrammetry. *Remote Sensing of Environment*, 209, 835-847.
- Van der Sluijs, J., Kokelj, S. V., Fraser, R. H., Tunnicliffe, J., & Lacelle, D. (2018). Permafrost terrain dynamics and infrastructure impacts revealed by UAV photogrammetry and thermal imaging. *Remote Sensing*, 10(11), 1734.
- Zefri, Y., ElKettani, A., Sebari, I., & Ait Lamallam, S. (2018). Thermal infrared and visual inspection of photovoltaic installations by UAV photogrammetry—application case: morocco. *Drones*, 2(4), 41.
- Edelman, G. J., & Aalders, M. C. (2018). Photogrammetry using visible, infrared, hyperspectral and thermal imaging of crime scenes. *Forensic science international*, 292, 181-189.
- Biass, S., Orr, T. R., Houghton, B. F., Patrick, M. R., James, M. R., & Turner, N. (2019). Insights into pāhoehoe lava emplacement using visible and thermal structure-from-motion photogrammetry. *Journal of Geophysical Research: Solid Earth*, 124(6), 5678-5695.
- Candiago, S., Remondino, F., De Giglio, M., Dubbini, M., & Gattelli, M. (2015). Evaluating multispectral images and vegetation indices for precision farming applications from UAV images. *Remote sensing*, 7(4), 4026-4047.
- Minařík, R., & Langhammer, J. (2016). USE OF A MULTISPECTRAL UAV PHOTOGRAMMETRY FOR DETECTION AND TRACKING OF FOREST DISTURBANCE DYNAMICS. *International Archives of the Photogrammetry, Remote Sensing & Spatial Information Sciences*, 41.
- Saura, J. R., Reyes-Menendez, A., & Palos-Sanchez, P. (2019). Mapping multispectral Digital Images using a Cloud Computing software: applications from UAV images. *Heliyon*, 5(2), e01277.
- Erenoglu, R. C., Akcay, O., & Erenoglu, O. (2017). An UAS-assisted multi-sensor approach for 3D modeling and reconstruction of cultural heritage site. *Journal of cultural heritage*, 26, 79-90.
- Raeva, P. L., Šedina, J., & Dlesk, A. (2019). Monitoring of crop fields using multispectral and thermal imagery from UAV. *European Journal of Remote Sensing*, 52(sup1), 192-201.
- Turner, R. M., MacLaughlin, M. M., & Iverson, S. R. (2020). Identifying and mapping potentially adverse discontinuities in underground excavations using thermal and multispectral UAV imagery. *Engineering Geology*, 266, 105470.